Numerical Simulation of High Lift Trapezoidal Wing with Transition Modeling in STAR-CCM+

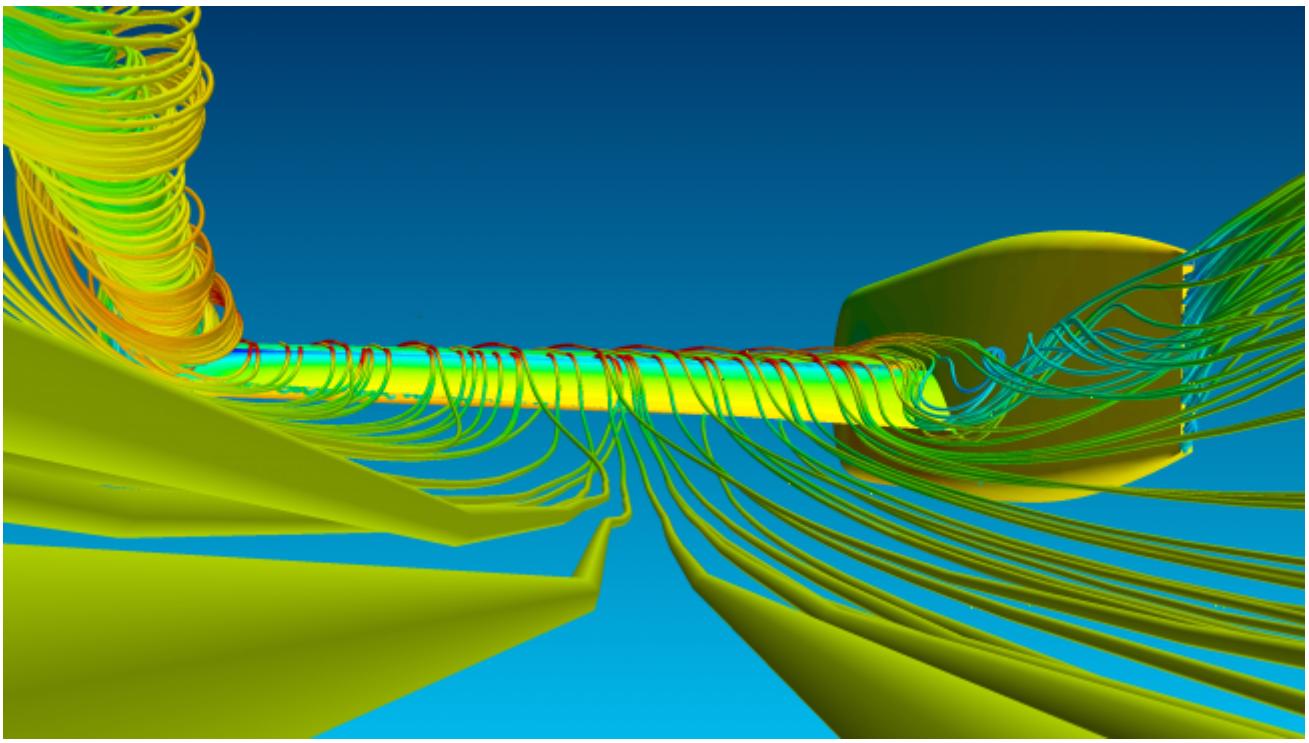

[1]

Prashanth Shankara,
CD-adapco

Geometry and test description

The geometry chosen for the validation of high lift prediction is the NASA Trapezoidal Wing geometry available in public domain. The trap wing (shown in geometry image) is a three element, high lift landing configuration with a slat deflection angle of 30 degrees and flap deflection angle of 25 degrees. Two more configurations, one with the flap at 20 degree deflection and another including flap brackets under the wing, will be simulated at a later stage. The three element wing consists of full span slat and flap, with a mean aerodynamic chord of 39.634 inches, aspect ratio of 4.561 and a semi-span of 85 inches.

The experiments on the trap wing were conducted in the 14x22 foot Subsonic Wind Tunnel at NASA Langley Research Center. The tests involved a semi-span model at a Reynolds number of 4.3 million, Mach No. of 0.2 and under free transition (i.e. no tripping mechanisms for transition). Pressure measurements were taken at over 700 surface locations but for the purpose of validating the numerical results, pressure coefficients at span-wise pressure tap rows (see pressure tap images) were given. A detailed summary of the experiments can be found on the H iLiftPW-1 website (www.hiliftpw.larc.nasa.gov [2]).

Computational mesh

The computational mesh was generated using the automatic meshing capability of STAR-CCM+ and the computational domain was discretized using polyhedral volume cells. Three grids of varying sizes referred to as coarse, medium and fine (see mesh images), were generated for a grid convergence study. Grid convergence was studied at the angles of attack, 13 and 28 degrees, as per the workshop guidelines. Grid sizes were 10 million, 22 million and 34 million. To accurately capture the flow in the boundary layer, a prism layer mesh consisting of hexahedral cells was created around the wing, with 25 layers of cells on the top, bottom and leading edge of the wing. The number of prism layers was reduced in areas like trailing edge and coves, where the boundary layer is not prominent. The coarse mesh solution was used to identify areas of flow where mesh refinement is required and the in-built 3D CAD Modeler of STAR-CCM+ was used to generate 3 dimensional objects of arbitrary shapes in these areas for refinement purposes. The Volumetric Refinement feature of STAR-CCM+ allows for specifying mesh sizes within the control volumes created in 3D CAD Modeler.

Solution using STAR -CCM+ and transition modeling

The simulations were carried out using CD-adapco?s flagship software, STAR-CCM+. STAR-CCM+ is an unstructured, cell centered, finite volume, Navier Stokes solver that has been well validated for a variety of aerospace applications. The boundaries of the computational domain were modeled as a freestream boundary with a Mach No. of 0.2 and Reynolds Number of 4.3 million based on Mean Aerodynamic Chord (MAC).

All simulations were computed using the steady state, coupled flow solver with implicit integration and second order discretization. Flow turbulence was modeled
using the SST (Menter) k-? turbulence model. The choice of the turbulent model was due to the fact that the y+ values, as instructed by the workshop committee,
were really low and the k-? model calculates the turbulence characteristics all the way to the wall without any numerical assumptions.

Another reason for the choice of this turbulence model was to facilitate the use of the correlation based Gamme Re-theta transition model in STAR-CCM+. The

transition model works only in conjunction with the SST (Menter) k-? turbulence model. The Langrty/Menter transition model in literature is incomplete due to the omission of two critical proprietary correlations. The Gamma Re-theta model in STAR-CCM+ uses internally specified correlations based on the data from Suluksna et. al and has been validated by Malan et. al. . Transition in the flow can be identified through a combination of intermittency and turbulence intensity plotted chord-wise. An example of transition identification from these two parameters is shown in the intermittency and turbulence images.

For the grid convergence study, all solutions were started from scratch and results showed that the coarse grid had the largest deviation from experimental results (around 4%). The final computations were run on all grids at seven different angles of attack: 6, 13, 21, 28, 32, 34 and 37. Force and moment coefficients were monitored to determine convergence. Computations were started without the transition model to achieve stability and then the transition model was invoked
to get to the final solution.

All simulations were initialized using the Grid Sequencing technique for faster convergence due to the relatively large CFL numbers that can be used. The Grid
Sequencing initialization follows up the normal initialization by computing an approximate inviscid solution by generating a series of coarse meshes from the
initial grid and computing solutions from the coarsest to the finest mesh.

Results

The lift, drag and pitching moment coefficients from STAR-CCM+ were compared to the values from the experiment at all seven angles of attack (see graphs). The numerical predictions from STAR-CCM+ agree well with the experimental data. At 37 degrees, prediction of lift becomes challenging due to massive separation and post-stall behavior. All three grids show good agreement with experimental data, with the accuracy of lift prediction increasing as the mesh becomes finer. The experiments show stall occurring at 36.1 degrees, while the CFD results show stall occurring between 36 and 37 degrees.

Good agreement with experimental results is also seen in the drag coefficient and pitching moment for all three grids (streamline images on the left). Below 28
degrees, drag coefficient prediction is excellent for all grids. Above 28 degrees, the fine mesh yields more consistent answers for drag coefficient with the test
data, although results from all grids are within the experimental error bounds. For the pitching moment coefficient prediction, a distinct improvement in predictions is seen with the medium mesh compared to other two grids. The discrepancy in prediction between the different grids is due to the different resolution of flap separation. The finest mesh predicts very little separation on the flap and gives the best results.

To gain more insight into the numerical prediction, surface pressure coefficients at various sections along the span are computed and compared against experimental data. A sample of the comparison at section cuts near root, mid-span and tip is shown below at 13 and 28 degrees. As expected, numerical predictions are excellent along root and mid-span but deteriorate towards the wing-tip. Wing-tip grid resolution and highly varying pressure gradients due to vortex roll-up from the wing-tips are a possible cause for under-prediction. Surface pressure prediction at slat shows excellent agreement with test data at all angles of attack.

Flow visualization at a surface and volume level was then used to identify the separation and

vortex formation behavior at different angles of attack. Surface streamlines show trailing edge separation along the flap span at lower angles of attack and this characteristic decreases as the angle of attack increases. At higher angles of attack, flow streamlines show very small trailing edge separation on the flap. Flow streamlines clearly show the increase in separation as the angle of attack increases.

Overall, the first round of simulations clearly show that STAR-CCM+ is able to capture most of the flow physics of the high-lift configuration. Future work will include further investigation of the wing-tip region, hysteresis effects, effect of support brackets and much more. The first step towards successfully validating STAR-CCM+ for high lift configurations has been completed. The latest/upcoming features of STAR-CCM+ such as body-fitted meshing and chimera grid will also greatly enhance the process/predictability of high lift aerodynamics.

References

K. Suluksna, P. Dechaumphai, and E. Juntasaro (2009), ?Correlations for Modeling Transitional Boundary Layers under Influences of Freestream Turbulence and Pressure Gradient?, International Journal of H eat and Fluid Flow, Vol. 30, pp. 66-75.
Malan P., Suluksna K ., Juntasaro E., (2009), ?Calibrating the Y-Re0 Transition Model for Commercial CFD?, AIAA-2009-1142-298, 47th AIAA Aerospace Science Meeting, Jan 2009

Industries:
Aerospace [3]
Aerospace - Sub-Industry [4]
Aircraft [5]
Products:
STAR-CCM+® [6]
Physics [7]
Turbulence [8]

Links:
[1] http://mdx2.plm.automation.siemens.com/case_study/numerical-simulation-high-lift-trapezoidal-wing-transition-modeling-star-ccm
[2] http://www.hiliftpw.larc.nasa.gov
[3] http://mdx2.plm.automation.siemens.com/industries/aerospace-defense
[4] http://mdx2.plm.automation.siemens.com/industries/aerospace-sub-industry
[5] http://mdx2.plm.automation.siemens.com/industries/aerospace/aircraft
[6] http://mdx2.plm.automation.siemens.com/products/star-ccm%C2%AE
[7] http://mdx2.plm.automation.siemens.com/products/physics
[8] http://mdx2.plm.automation.siemens.com/products/star-ccm%C2%AE/turbulence